

Astrocytes from old Alzheimer's disease mice are impaired in A β uptake and in neuroprotection



Tal Iram^{a,b}, Dorit Trudler^{a,b}, David Kain^a, Sivan Kanner^a, Ronit Galron^a, Robert Vassar^c, Ari Barzilai^{a,b}, Pablo Blinder^{a,b}, Zvi Fishelson^d, Dan Frenkel^{a,b,*}

^a Department of Neurobiology, George S. Wise Faculty of Life Sciences, Tel Aviv University, Tel Aviv, Israel

^b Sagol School of Neuroscience, Tel Aviv University, Tel Aviv, Israel

^c Department of Cell and Molecular Biology, Feinberg School of Medicine, Northwestern University, Chicago, IL 60611, USA

^d Department of Cell and Developmental Biology, Sackler School of Medicine, Tel Aviv University, Tel Aviv 69978, Israel

ARTICLE INFO

Article history:

Received 26 February 2016

Revised 11 July 2016

Accepted 16 August 2016

Available online 17 August 2016

Keywords:

Adult astrocyte culture

Alzheimer's disease

Neurotoxicity

A β uptake

SR-B1

VEGF

C1q

ABSTRACT

In Alzheimer's disease (AD), astrocytes undergo morphological changes ranging from atrophy to hypertrophy, but the effect of such changes at the functional level is still largely unknown. Here, we aimed to investigate whether alterations in astrocyte activity in AD are transient and depend on their microenvironment, or whether they are irreversible. We established and characterized a new protocol for the isolation of adult astrocytes and discovered that astrocytes isolated from old 5xFAD mice have higher GFAP expression than astrocytes derived from WT mice, as observed *in vivo*. We found high C1q levels in brain sections from old 5xFAD mice in close vicinity to amyloid plaques and astrocyte processes. Interestingly, while old 5xFAD astrocytes are impaired in uptake of soluble A β 42, this effect was reversed upon an addition of exogenous C1q, suggesting a potential role for C1q in astrocyte-mediated A β clearance. Our results suggest that scavenger receptor B1 plays a role in C1q-facilitated A β uptake by astrocytes and that expression of scavenger receptor B1 is reduced in adult old 5xFAD astrocytes. Furthermore, old 5xFAD astrocytes show impairment in support of neuronal growth in co-culture and neurotoxicity concomitant with an elevation in IL-6 expression. Further understanding of the impact of astrocyte impairment on AD pathology may provide insights into the etiology of AD.

© 2016 Elsevier Inc. All rights reserved.

1. Introduction

Astrocytes have paramount importance in the development, maintenance and repair of the neural environment (Attwell et al., 2010; Kofuji and Newman, 2004; Pellerin et al., 2007; Rothstein et al., 1996). It is becoming widely accepted that astrocyte dysfunction underlies many diseases of the nervous system, such as Alzheimer's disease (Sofroniew and Vinters, 2010; Verkhratsky et al., 2014). Alzheimer's disease (AD) is a progressive neurodegenerative disorder characterized by an accumulation of senile plaques and neurofibrillary tangles (NFTs) containing the β -amyloid (A β) peptide and the hyperphosphorylated microtubule-associated protein tau, respectively (Braak et al., 1993). Most cases of AD are sporadic, while <5% of cases are early onset familial Alzheimer's disease (FAD) with autosomal dominant gain of function mutations in the Amyloid Precursor Protein (APP) and Presenilin1 (PS1) genes, that increase the production of A β (Goldman et al., 2002).

Rodriguez and colleagues demonstrated that astrocyte morphology in AD is remarkably heterogeneous and dependent on the interaction with A β , brain region and disease state (Kulijewicz-Nawrot et al., 2012; Olabarria et al., 2010; Yeh et al., 2011). They found substantial atrophy of astrocytes not associated with plaques, which was apparent even before plaque formation and remained until the late stages of the disease. They postulated that the retraction of astrocytic processes from the synapse could result in defective synaptic modulation and subsequently lead to cognitive defects in AD. These observations point toward an early imbalance in astrocytic function in AD.

Impairment in astrocyte function in AD was further demonstrated in the transcriptional level by Hol and colleagues, who performed a full transcript analysis of cortical astrocytes from an aged mouse model of AD (APP^{swe}PS1^{dE9}) compared to age-matched control astrocytes. Interestingly, 20% of the astrocyte specific genes were downregulated, as opposed to 6% upregulated genes, indicating an overall impairment of healthy astrocytic functions. Many of the downregulated genes were classified to gene clusters linked to neuronal support and neuronal communication (Orre et al., 2014a).

It is hypothesized that an overall impairment in A β clearance leads to the imbalance between A β production and clearance and subsequently results in A β accumulation and disease progression (Bateman

* Corresponding author at: Department of Neurobiology, George S. Wise Faculty of Life Sciences, Tel Aviv University, Tel Aviv, Israel.

E-mail address: dfrenkel@post.tau.ac.il (D. Frenkel).

Available online on ScienceDirect (www.sciencedirect.com).

et al., 2006; Mawuenyega et al., 2010). It was reported that astrocytes can accumulate A β *in vivo*, and express a wide variety of phagocytic receptors and enzymes, which may promote A β degradation, positioning them as major scavenging cells in the brain (Cahoy et al., 2008; Iram and Frenkel, 2012; Mulder et al., 2012; Thal et al., 2000). In addition, astrocytes express different scavenger receptors that are important for apoptotic cell removal (Iram et al., 2016), specifically scavenger receptor B1 (SR-B1) (Alarcon et al., 2005; Sofroniew, 2009), which can also mediate A β uptake (Alarcon et al., 2005; Husemann et al., 2002). Interestingly, A β uptake and degradation seems to be a unique characteristic of adult astrocytes but not neonatal astrocytes in rodents (Wyss-Coray et al., 2003). Thus, a continuous reduction in astrocyte-mediated debris clearance mechanisms might exacerbate the amyloid pathology in AD.

Complement components, like C1q and C3, are present in elevated levels in AD in association with plaques (Eikelenboom and Stam, 1984). C1q can bind A β directly and enhance A β aggregation (Jiang et al., 1994). Deletion of C1q in an AD mouse resulted in significantly lower activation of glia around plaques and less neuronal and synaptic toxicity (Fonseca et al., 2004). However, the precise mechanism of interaction between C1q and astrocytes in AD is not known.

In this study, we aimed at determining whether old 5xFAD astrocytes were permanently affected following long-term exposure to the AD brain environment. We found that old 5xFAD astrocytes cultured *in vitro* maintained GFAP overexpression and were functionally impaired in A β uptake and in neuronal support. Our data suggests a role for C1q in mediating astrocyte activity in AD.

2. Methods

2.1. Mice

The AD mouse model used in this experiment is 5xFAD mouse model expressing five FAD mutations in APP and PS1 as previously described (Oakley et al., 2006). Experiments were done on young (3 months) or old (12–14 months) 5xFAD or littermate-control mice. All animal care and experimental use was in accordance with the Tel Aviv University guidelines and was approved by the Tel Aviv University Animal Care Committee.

2.2. Adult astrocyte culture

Mice were sacrificed in CO₂ and perfused with cold PBS. Brains (cerebellum and brain stem excluded) were dissociated to single cell suspensions using a papain-based neural dissociation kit following the manufacturer's instructions (Miltenyi Biotech). Myelin was removed using a Percoll gradient (Sigma), after two washing steps, red blood cells were lysed and the remaining cells were plated on Poly-D-Lysine (PDL)-coated 12-well plates at a concentration of 7.5×10^5 cells/well (1.2×10^5 cells/cm²) or used as a whole brain single cell-suspension in flow cytometry experiments. Cells were grown with complete astrocyte medium (ScienCell) for 2–3 weeks, passaged once on day 7 *in vitro* (DIV7) and a second and a final passage at DIV10 (1:3 or 1:6 ratio, respectively). Before the second passaging, plates were placed on a shaking rotator (120 rpm) for 2 h at 37 °C. At 12–20 DIV, cell purity was assessed and subsequent experiments were conducted. Cells were detached for passaging with 0.05% Trypsin-EDTA (Gibco).

2.3. Flow cytometry

For intracellular GFAP staining, astrocyte cultures were washed and detached in a non-enzymatic manner, spun and resuspended in a cell permeabilization/fixation buffer for 30 min on ice (R&D biosciences), washed in PBS and then blocked in a permeabilization buffer (R&D biosciences) containing 1% FCS and 10% Fc Blocker solution (Miltenyi Biotech) for 10 min at RT. Mouse-anti-GFAP-Alexa-488 antibody (1:20, BD Biosciences Cat# 560297, RRID:AB_1645350) was added to the

blocking solution for 30 min. For anti-CD11b (microglial cell marker) staining, astrocyte cultures were washed and detached in a non-enzymatic manner and a whole brain single cell suspension was incubated with 10% Fc Blocker solution (Miltenyi Biotech) for 10 min at RT following staining with rat-anti-CD11b-PE (1:100, BD Pharmingen) for 20 min on ice. Cells were washed and antigen expression was determined using Becton Dickinson FACSsort and Cyflogic software.

2.4. Immunostaining

Astrocytes were plated on Poly-D-Lysine (PDL)-covered 12 mm cover slips for 48 h. Fresh-frozen 4-month-old and 15-month-old WT and 5xFAD brains were sectioned in a cryostat to 12 μ m sections and mounted on slides. Slides were kept at -80 °C until staining. Slides and coverslips were washed and fixed with 4% PFA for 10 min, blocked in blocking medium (8% Horse serum, 0.3% Triton, 1 g/100 ml BSA, 88.7% PBS, 0.02% Sodium Azide) for 30 min. Next, they were incubated with primary antibodies; rabbit-anti-GFAP (1:500, Sigma-Aldrich Cat# G9269, RRID:AB_477035), mouse-anti-S100 β (1:100, Sigma), rabbit-anti-IBA1 (1:500, Wako Cat# 019-19741, RRID:AB_839504), rat-anti-CD31 (1:500, BD Biosciences Cat# 550274, RRID:AB_393571), mouse-anti-A β (6E10, 1:750, Covance), mouse-anti- β -tubulin (1:500, Millipore), and mouse-anti-C1q (1:200, Abcam) in blocking medium overnight at 4 °C, then washed with PBS and incubated with matching secondary antibody (1:500, Alexa-488, Invitrogen) for 1 h at RT. All the staining was compared to staining by secondary antibody alone. Congo red staining (Sigma) was done after secondary staining, as previously described (Lifshitz et al., 2013). Cover slips were mounted on slides with Vectashield including DAPI nuclear stain (Vector laboratories) and visualized in a Nikon Eclipse ME600 fluorescent microscope equipped with a high resolution DXM1200C Nikon digital camera or in a Zeiss LSM META confocal microscope as indicated. Using confocal microscopy, we imaged astrocytes from cortices of young and old 5xFAD mice and reconstructed the surface volume (surface rendering) of the astrocytes and 6E10 by IMARIS software V7.1.1 (Imaris, RRID:SCR_007370). This enabled us to calculate the volume of internalized 6E10 inside GFAP volume as was previously done for microglial engulfment (Schafer et al., 2014; Schafer et al., 2012). Quantification of uptake was done by dividing the internalized 6E10 volume by total GFAP volume and total 6E10 volume to account for the increase of both GFAP and A β 42 with age.

2.5. Real-time PCR analysis

Total RNA was extracted from cultured astrocytes and brain homogenates (excluding cerebellum) using the MasterPure™ RNA Purification Kit (Epicentre). SYBR Green real-time PCR primers were purchased from Agentek (Tel Aviv, Israel). RT-PCR was performed with primers specific for GFAP, GS, S100 β , CD31, CD11b, synaptophysin, MBP, C1qA, SRA, SR-B1 BDNF, NTF3, VEGFa and IL6 using an Applied Biosystems PRISM 7300 thermal cycler as previously described (Trudler et al., 2014).

2.6. ELISA

Astrocyte cultures were stimulated with or without 5 μ g/ml Polyinosinic:polycytidylic acid (Poly I:C, Sigma) in serum-free astrocytes medium for 24 h (Park et al., 2006). IL-6 cytokine levels were measured in cell supernatant by quantitative ELISA, using paired antibodies and recombinant cytokines according to the manufacturer's recommendations (BD PharMingen Systems), as previously described (Trudler et al., 2014).

2.7. Western blot analysis

Western blot was done as previously described (Trudler et al., 2014). In brief, a lysis buffer was added to each well, and samples were

collected and shaken for 20 min on ice, transferred to 1.5 ml tubes and centrifuged for 20 min at 10,000g at 4 °C. Finally, the supernatants were transferred to new 1.5-ml tubes and stored at –70 °C. Protein concentrations were determined using Bradford reagent (Bio-Rad Laboratories). For electrophoretic separations, 10% polyacrylamide gels were used. Samples were transferred to nitrocellulose membranes. The membranes were blocked with 5% bovine serum albumin block buffer for 1 h, washed with 0.05% Tween in TBS (TBST), and reacted with rabbit anti-GFAP (1:5000, Sigma-Aldrich Cat# G9269, RRID:AB_477035) overnight at 4 °C. The membranes were washed three times with PBS-Tween (0.05%) and reacted with secondary goat-anti-rabbit-HRP (1:10,000, Jackson) for 1 h at 25 °C. The membranes were washed with TBST, reacted with ECL and measured using the Amersham imager 600UV (GE life technologies). Mouse anti-glyceraldehyde 3-phosphate dehydrogenase antibody (GAPDH, 1:10,000, Millipore Cat# MAB374, RRID:AB_2107445) was used as a loading control.

2.8. A β uptake by flow cytometry

Adult astrocytes were cultured in 12-well plates and incubated with 0.12 μ M Alexa-488 labeled A β 42 mounts (AnaSpec) at 37 °C as previously described (Farfara et al., 2011). In the C1q experiments, 0.12 μ M Alexa-488 labeled A β 42 was incubated with indicated amounts of C1q (1–10 μ g/ml C1q) (Complement Technologies Inc., #A099) or a C1q diluent buffer as control (10 mM HEPES, 300 mM NaCl, in DDW, pH = 7.4) for 30 min at 37 °C and then placed over the astrocyte cultures for 2 h. In fucoïdan experiments, fucoïdan (Sigma, F5631) was pre-incubated on cells in indicated amounts (100 μ g/ml) for 30 min at 37 °C and then the A β and C1q were added for 2 h as described above (Husemann et al., 2002).

2.9. C1q fluorescence labeling and uptake

Recombinant C1q (Complement Technologies Inc.) was labeled using a 5-FAM protein labeling kit following the manufacturer's instructions (Anaspec, #AS-72053). Briefly, C1q was mixed with the dye in a molar ratio of 10:1 and shaken on a rotator for 1 h. Unbound dye was removed using a size separation column. For the uptake experiments, adult WT and 5xFAD astrocytes were cultured on coverslips and incubated overnight (16 h) with 0.2 μ M Alexa-488 labeled A β 42 (AnaSpec) preincubated with 10 μ g/ml un-labeled C1q, 10 μ g/ml 5-FAM labeled C1q or control buffer (Complement technologies) at 37 °C for 30 min. Cells were washed, fixed with 4% PFA and then stained with anti-GFAP antibodies following the procedure described in Section 2.4. Imaging was done using a Zeiss LSM META confocal microscope.

2.10. Open craniotomy and two-photon microscopy

Mice were anesthetized with Isoflurane (5% for induction, 1%–2% thereafter) and carprofen (5 mg/kg) was given as analgesia. The scalp and connective tissue were removed, and the dry skull was covered with cyanoacrylamide (Gdalyahu et al., 2012). A 3-mm diameter craniotomy was done and 0.2 μ M Alexa-488 labeled A β 42 (AnaSpec) was locally pressure-ejected from a micropipette in 50 μ m increments up to 500 μ m deep. For *in vivo* labeling of cortical astrocytes, SR101 (Thermo Scientific, #S359) was dissolved in artificial CSF to a concentration of 100 μ M and applied directly to the exposed neocortical surface for 4 min and then rinsed extensively (Nimmerjahn et al., 2004). The cranial window was covered with a custom-made 3 mm coverglass (Bellco Glass) and sealed with cyanoacrylamide. The dry glue was covered with Dental Acrylic. An aluminum metal bar with two traded holes was attached to the skull with black Dental Acrylic. Imaging was conducted with a custom-modified two-photon laser-scanning microscope based on a Sutter MOM (Sutter Inc) controlled through the MPScope 2.0 software system (Nguyen et al., 2009). SR101 and A β 42 were imaged using 820 nm excitation and a 25 \times objective. Time lapse imaging of

50 μ m z-stacks (with 0.4 μ m step) was obtained every minute for 20–30 min. During the surgery and imaging session, the temperature of the mice was kept at 37 °C and 100 μ l 5% sucrose was administered hourly. 4D reconstruction of the SR101 and A β 42 surface over time was done using Imaris V7.1.1 (Imaris, RRID:SCR_007370).

2.11. Neonatal neuronal culture

Neuronal isolation was done as previously described (Lavi et al., 2014). Cortical neuronal cultures were prepared from P1 and P2 newborn mice. Briefly, cortices from five P1–2 BALB/c pups were dissected and placed on ice, chopped with scissors in a papain based dissociation buffer (2.5 mM CaCl₂, 0.83 mM EDTA, 137 U papain (Sigma), 100 μ l DNase (Sigma), 3–5 crystals of Cysin HBSS–Hepes (20 mM)) and placed on a rotating shaker for 20 min at RT and spun down. The pellet was re-suspended with growth medium (5% FCS, 2% B27, 1% L-Gln, 0.5% Pen-Strep in Neurobasal A medium) and triturated seven times. Cells were placed in a 10 mm dish for 1 h at 37 °C and supernatant containing neurons, was spun and used for co-culture experiments. A total of 1.5×10^5 cells in 1 ml growth medium were plated on each astrocyte well for 24 h.

2.12. N2A cell culture

Neuroblastoma 2A cells were cultured in 48-well plates at a concentration of 3.5×10^5 cells/well for 24 h prior to stress induction. The N2A cells were grown in DMEM supplemented with 1 mM sodium pyruvate, 4 mM L-glutamine, 10% FCS, 100 U/ml penicillin, 0.1 mg/ml streptomycin (Biological Industries, Beit-Haemek, Israel). To induce cell death, N2A cells were exposed to 300 μ M of H₂O₂ in serum-free medium for 4 h. The medium was replaced, and the cells were left to recover in astrocyte-conditioned media for 24 h. Cell survival was evaluated using methylene blue (3,7-bis(Dimethylamino)-phenazathionium chloride; Sigma #M9140) staining (Yamazaki et al., 1986), with minor modifications. The N2A culture was fixed using 200 μ l of 4% formaldehyde in PBS for 2 h. The cells were then washed with 0.1 M boric acid for 10 s. A total of 200 μ l of 1% methylene blue in 0.1% boric acid was placed in the wells for 20 min. The cells were washed three times with water. The color was eluted from the cells with 200 μ l of 0.1% HCl, 100 μ l of the solution was placed into a 96-well plate, and light absorption at 595 nm was measured with a spectrophotometer.

2.13. Statistical analysis

Data comparisons were carried out using a two-tailed Student's *t*-test for two groups and one-way ANOVA following a Bonferroni post-hoc test for multiple group comparisons using Graphpad Prism software. *p*-Values <0.05 were considered statistically significant.

3. Results

3.1. Generation of astrocyte cultures from adult mice

In order to investigate alterations in astrocytes from young and old 5xFAD mice, we established a new protocol for adult astrocyte culture. Cell culture purity was assessed using flow cytometry, immunofluorescence staining and gene expression by RT-PCR. Flow cytometry quantification of GFAP protein, a known astrocyte marker, showed that >95% of the population is GFAP positive (Fig. 1A–B). Since the presence of microglial cells tends to affect the cytokines profile (Stellwagen and Malenka, 2006), we examined the presence of microglia in astrocyte cell culture and in the whole brain by anti-CD11b staining. We found that while there is an average of 11.6% CD11b-positive cells in whole brain, in our astrocyte cell culture this percentage dropped to 1.5% CD11b-positive cells (*p* < 0.001, Fig. 1C–D). We further validated our astrocyte cell culture purity by immunofluorescence staining with

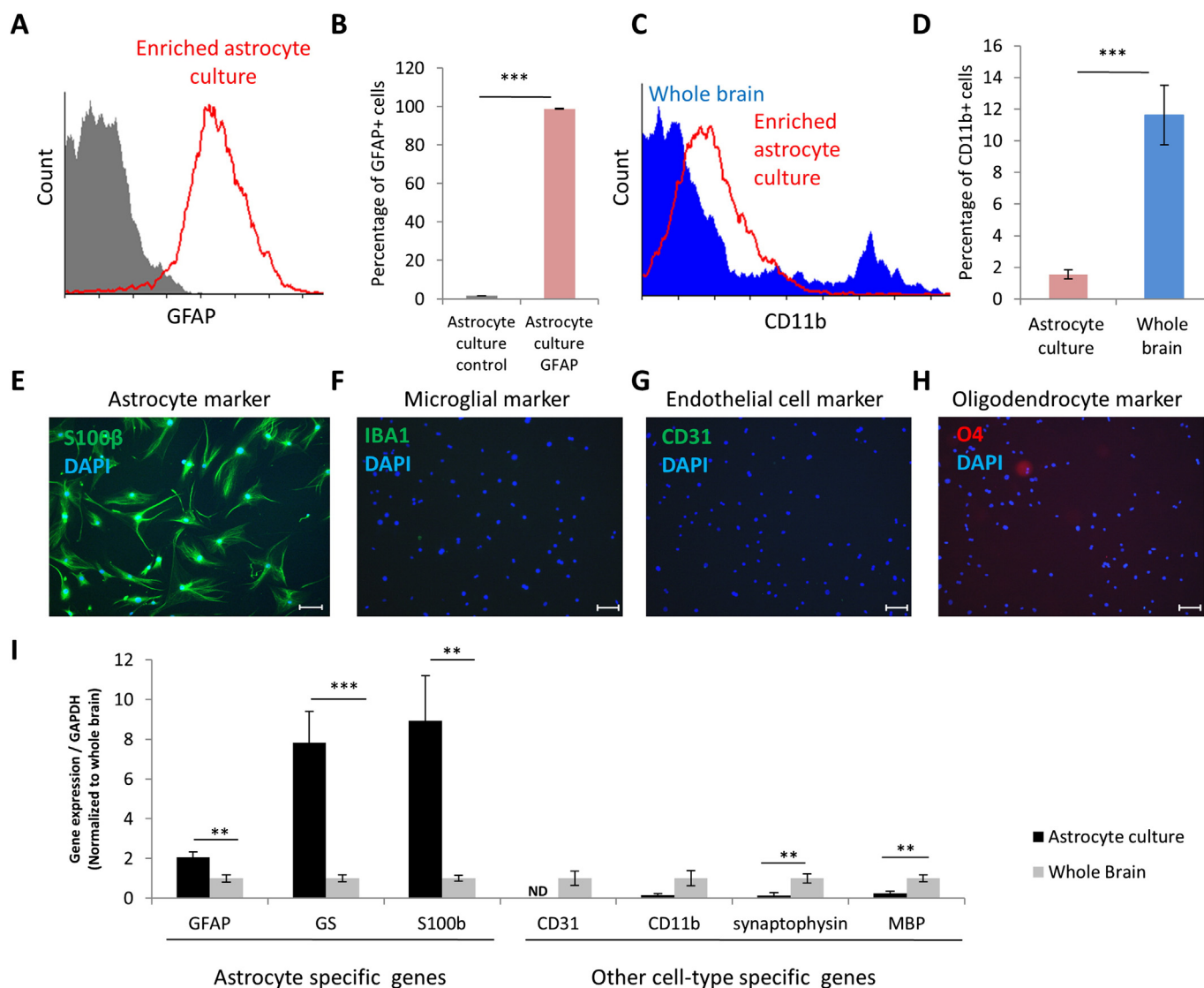


Fig. 1. Generation of adult astrocyte cell culture. (A–B) Quantification of percentage of GFAP positive cells in the astrocyte culture by flow cytometry (Representative of 3 independent experiments done in triplicates, $n = 3$). (C–D) Comparison between percentage of CD11b positive cells by FACS from whole-brain single cell suspension before culture and in astrocyte culture. (E–H) Cultured astrocytes were plated on coverslips and stained for cell-specific markers (E) S100 β , (F) IBA1, (G) CD31 and (H) O4 for detection of astrocytes, microglia, endothelial cells and oligodendrocytes, respectively (representative images of 3 independent cultures). (I) Cell specific genes were measured by RT-PCR in astrocyte culture compared to expression levels in whole brain homogenates ($n = 3$). Error bars represent mean + SEM, ** $p < 0.01$, *** $p < 0.001$, ND - not detected.

another astrocyte-specific marker; S100 β (Fig. 1E) and other cell-type specific markers for microglia (IBA1, Fig. 1F), endothelial cells (CD31, Fig. 1G) and oligodendrocytes (O4, Fig. 1H). We found that >99% of the cells were stained with S100 β with no clear evidence for any other cell types. We further evaluated our cell culture using RT-PCR by targeting specific cell markers such as: astrocytes (GFAP, Glutamine synthetase, S100 β), endothelial cells (CD31), microglia (CD11b), neurons (synaptophysin) and oligodendrocytes (MBP) (Fig. 1I). We found that cultured astrocytes had an enriched expression of astrocyte specific genes and low expression of other cell type specific genes compared to whole brain. Altogether, these experiments show that our culture protocol generates a highly enriched adult astrocyte culture.

3.2. Astrocytes from old 5xFAD mice cultured in vitro maintain GFAP upregulation

We used the 5xFAD mouse model that is characterized by accelerated amyloid pathology and memory impairments already at 4 months of age (Oakley et al., 2006). As shown in Fig. 2, brain slices from old 5xFAD mice (12–14 months), express high levels of GFAP (red staining) in

regions with extensive A β plaque load (green staining) as compared to age-matched control mice (Fig. 2A–B). We further quantified differences in astrocyte activation by the analysis of GFAP gene expression levels by RT-PCR ($p < 0.05$, Fig. 2E) and by Western blotting ($p < 0.01$, Fig. 2F) in whole brain homogenates. In cultured astrocytes, we found that GFAP expression remained higher in astrocytes isolated from old 5xFAD mice vs. control as measured by GFAP immunostaining (Fig. 2C–D), mRNA levels ($p < 0.05$, Fig. 2G) and WB ($p < 0.001$, Fig. 2H).

3.3. Astrocytes from old 5xFAD mice have less internalized A β in vivo and impaired A β uptake in vitro

To examine the ability of adult astrocytes to uptake A β *in vivo*, we injected fluorescently labeled A β 42 to the cortex of a 4-month-old 5xFAD mouse using a micropipette through an open cranial window. Astrocytes were labeled by surface application of SR101 as was previously described (Nimmerjahn and Helmchen, 2012; Nimmerjahn et al., 2004). Two hours after injection, fluorescent A β 42 could be found within astrocyte cell bodies and processes (Fig. 3A–C). Time-lapse imaging of astrocyte z-stacks showed the dynamics of the uptake process in

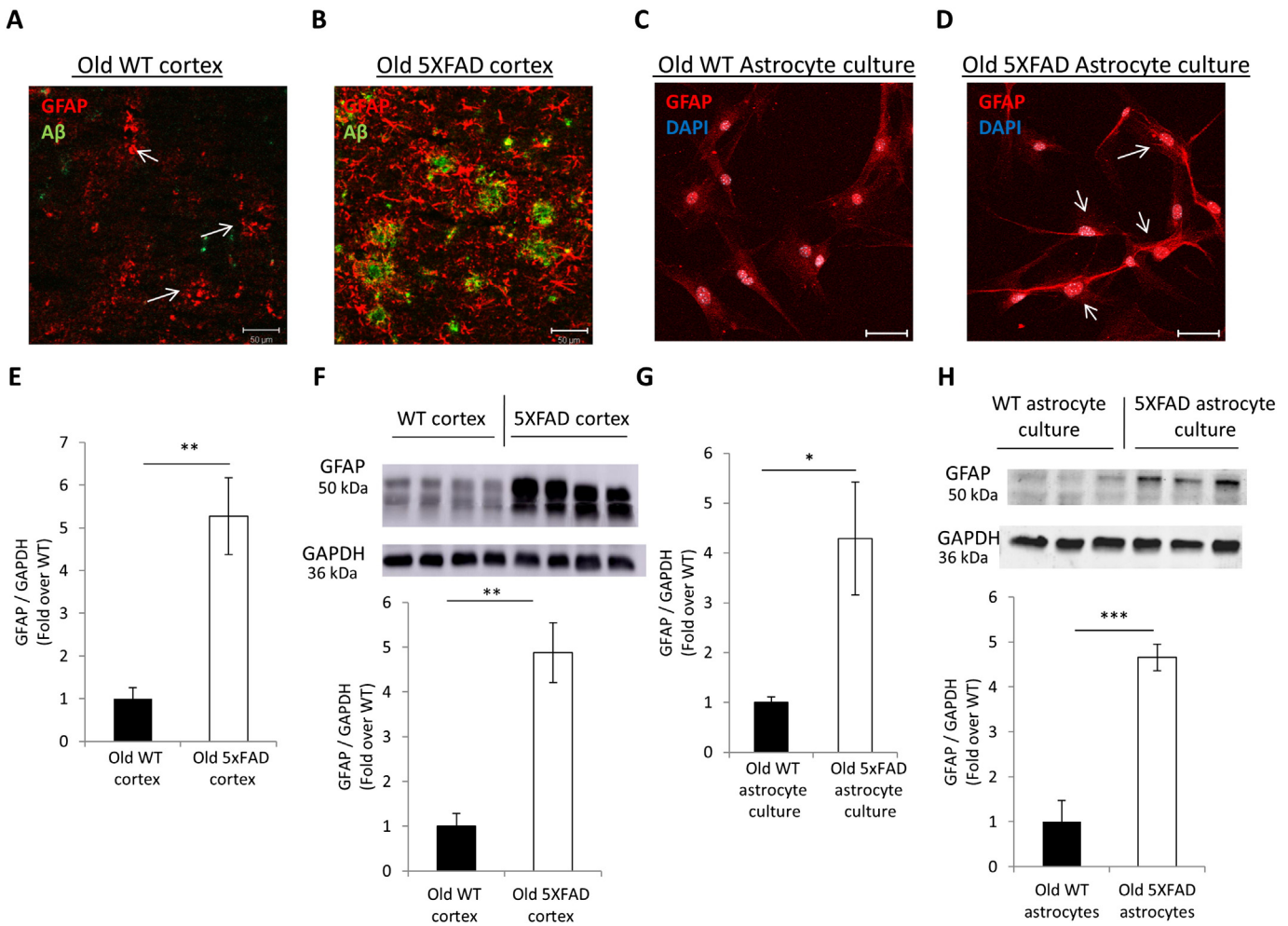


Fig. 2. Old 5xFAD astrocytes display GFAP upregulation in culture. (A–B) Coronal slices from 14-month-old (A) WT and (B) 5xFAD mice were stained with antibodies against GFAP (red), Aβ42 (6E10, green) and DAPI (blue) and imaged by confocal microscopy. Scale bar represents 50 μm (n = 3). (C–D) WT and 5xFAD astrocytes from 12-month-old mice in culture stained with antibodies against GFAP (red) and DAPI (blue). Scale bar represents 50 μm (n = 3). (E–F) GFAP expression levels were measured in whole cortex extracts from 12-month-old WT and 5xFAD mice by (E) RT-PCR and (F) Western blot (n = 9). (G–H) GFAP expression levels were measured in astrocyte culture of 12-month-old WT and 5xFAD mice by (G) RT-PCR (n = 8–10) and (H) Western blot (n = 3, representative blot of 3 independent cultures in triplicates). Error bars represent mean + SEM, *p < 0.05, **p < 0.01, ***p < 0.001.

the same astrocyte for 20 min (Supplementary Fig. 1 and Movie 1). To measure astrocyte Aβ uptake during disease progression *in vivo*, we stained coronal sections of young (4 months) and old (15 months) 5xFAD brains for Aβ and GFAP. We quantified Aβ internalization using the IMARIS software and discovered that old 5xFAD astrocytes internalized 35% less Aβ compared to young 5xFAD (Fig. 3D–J). We further assessed whether this effect can be seen in adult astrocytes *in vitro*. We found that while young WT and 5xFAD astrocytes did not differ in their ability to phagocytose fluorescent Aβ42 measured by flow cytometry, old 5xFAD astrocytes showed a 20% lower Aβ42 uptake compared to old WT astrocytes (p < 0.001, Fig. 3K), reproducing the deficiency *in vivo*. Interestingly, this appears to be a general impairment in uptake, as old 5xFAD astrocytes showed a substantial reduction in latex beads uptake compared to old WT astrocytes as measured by flow cytometry (Supplementary Fig. 2).

3.4. Old 5xFAD astrocytes are associated with C1q and Aβ plaques

C1q is an initiator of the classical complement pathway and its levels were reported to be increased in AD brains (McGeer and McGeer, 2002). C1q was found to be associated with Aβ plaques (Eikelenboom and Stam, 1984) and linked to the neurodegeneration process in AD (McGeer and McGeer, 2002). We stained brain slices of old 5xFAD with mouse anti-C1q (red) and rabbit anti-GFAP (green) antibodies

combined with Congo red that stains β-sheet protein structures found in dense Aβ plaques (white, Fig. 4A–B). z-Stack analysis of confocal images revealed that C1q localized with Aβ plaques and with astrocyte processes surrounding the plaques (Fig. 4C–D). We found an increased expression of C1qA, one of the C1q subunits, in the cortex of AD mice at 6 months, when there is a profound appearance of Aβ plaques in this model (Fig. 4E).

While it was previously suggested that the majority of brain C1q is expressed by microglia (Stephan et al., 2013), we discovered that adult old 5xFAD astrocytes in cell culture were positively stained for C1q (Fig. 4F). Interestingly, C1qA levels were increased in old 5xFAD astrocytes by about 2.5-fold over C1q expression in old WT astrocytes (p < 0.05, Fig. 5G). This difference could not be detected in young astrocytes (Fig. 4H) indicating that astrocyte impairment might occur upon exposure to the diseased environment.

3.5. C1q-enhanced Aβ uptake by astrocytes involves a scavenger receptor-dependent pathway

While complement activation was suggested to play a detrimental role in AD, it was also previously suggested that C1q may increase Aβ uptake by microglia (Fraser et al., 2010). To measure the effect of C1q on Aβ uptake by astrocytes in culture, fluorescently labeled Aβ42 was pre-incubated with C1q and then placed on old 5xFAD astrocyte

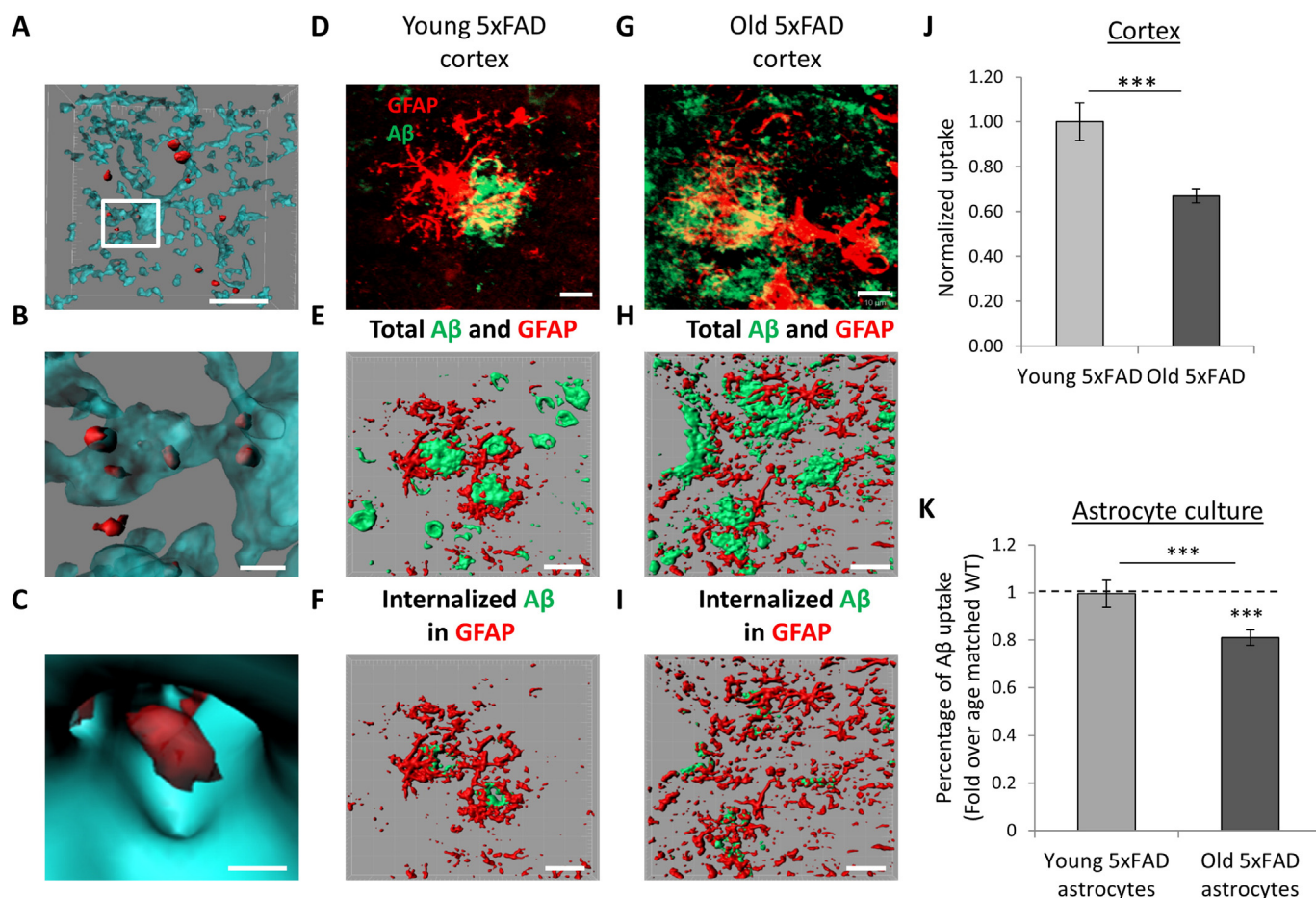


Fig. 3. Old 5xFAD mice astrocytes demonstrate reduced A β -internalization compared to control *in vivo* and *in vitro*. (A–C) Representative 3D surface rendering of astrocyte (cyan) and A β 42 (red) following 2 h injection of A β to mouse cortex imaged by *in vivo* two photon microscopy. (A) Whole cell, (B) magnification of a process showing internalized A β and (C) fully internalized A β within an astrocyte process. (For full time lapse movies, see supplementary material). (D–I) Coronal slices from (D–F) 4-month-old 5xFAD and (G–I) 15-month-old 5xFAD mice were stained with antibodies against astrocytes (GFAP, red) and A β (6E10, green) and imaged by confocal microscopy. (D, G) Representative 3D projection of one astrocyte in association with 6E10 positive amyloid plaques. Scale bar represents: (A, D, G) 10 μ m, (B) 1 μ m, (C) 0.2 μ m, (E, H, F, I) 50 μ m. (E, H) Representative surface rendering of total GFAP (red) and total 6E10 (green) staining. (F, I) Representative surface rendering of total GFAP (red) and internalized 6E10 (green) staining. (J) Quantification of internalized A β in astrocytes in young and old 5xFAD mice. (n = 3 mice/age, 10–15 images per mouse, Student *t*-test, ****p* < 0.001). (K) Young and old WT and 5xFAD astrocyte cultures were incubated for 2 h with fluorescently-labeled soluble A β and uptake was measured by Flow cytometry. Percentage of uptake by young 5xFAD (n = 14) was normalized to young WT astrocytes (n = 12, run in two independent experiments in quadruplicates, not significant) and of old 5xFAD astrocytes to old WT astrocytes (n = 14–18, run in six independent experiments in triplicates, ****p* < 0.001). Normalized uptake A β was compared between young and old 5xFAD astrocytes (n = 16–18, Student *t*-test, *p* < 0.001).

cultures. We discovered that incubation of A β with C1q increased A β uptake, as shown by immunostaining and by FACS (Fig. 5A, B and F). To assess whether A β and C1q interact directly to affect A β uptake, we pre-labeled C1q fluorescently with 5-FAM (green) and repeated the experiment with fluorescently labeled A β 42 (magenta). Confocal images confirmed that C1q was co-localized with A β (white) (Fig. 5C–E). We discovered that there were also A β fragments that were taken up in C1q-independent manner. Quantitative analysis by FACS shows an increase in C1q-dependent A β uptake in a dose-response manner. It was previously suggested that scavenger receptors facilitate A β uptake by astrocytes (Alarcon et al., 2005; Husemann et al., 2002). It was also suggested that there is a link between scavenger receptors to C1q in astrocytes (Mulder et al., 2012). To evaluate the contribution of scavenger receptors to C1q activity, we used fucoidan, a known scavenger receptor ligand (Husemann et al., 2002) in a competition assay. We discovered that fucoidan significantly reduced the effect of C1q on A β uptake in astrocytes (*p* < 0.001, Fig. 5F). Nevertheless, we discovered that there is an elevation in A β uptake with a higher dose of C1q incubated together with fucoidan (*p* < 0.05), which suggests the involvement of other C1q receptors in this process.

To investigate the difference between WT to 5xFAD astrocytes, we focused on two known astrocyte scavenger receptors: scavenger

receptor A (SR-A) and scavenger receptor B1 (SR-B1) expression (Alarcon et al., 2005; Sofroniew, 2009). We discovered that old 5xFAD astrocytes, but not young 5xFAD astrocytes, had reduced SR-B1 (*p* < 0.05, Fig. 5G). Interestingly, there was no significant difference in SR-A expression between WT and 5xFAD astrocytes from young and old mice (Fig. 5G). This result suggests that C1q-mediated impairment of A β uptake by astrocytes might be due to the reduction in expression of SR-B1.

3.6. Old 5xFAD astrocytes have impaired ability to promote neuronal growth

Given the extensive dependency of neurons on astrocytic support for their growth and viability, we used neuron-astrocyte co-cultures to investigate whether old 5xFAD astrocytes were impaired in the promotion of neurite growth. We isolated neurons from P1–P2 pups and plated them on confluent old WT or 5xFAD astrocytes cultured on coverslips. Length of the longest neurite per neuron, evident by β -tubulin staining, was measured in at least 100 neurons per coverslip. We discovered that old 5xFAD astrocytes promoted growth of shorter neurites as compared to old WT astrocyte cultures (*p* < 0.05, Fig. 6A–C). Previous research has indicated that astrocytes isolated from AD mouse models

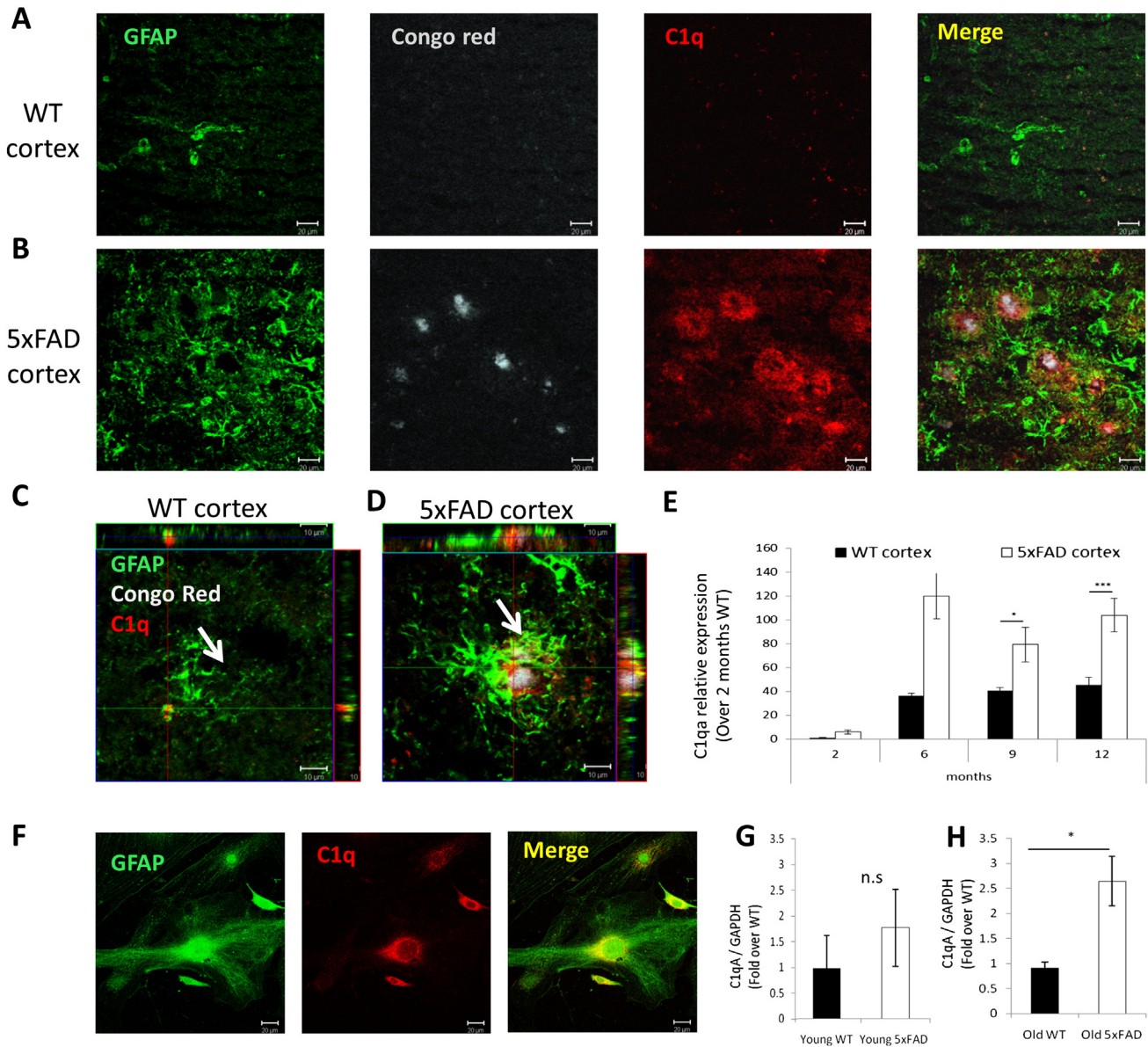


Fig. 4. Old 5xFAD astrocytes associate with C1q and A β plaques. (A–D) Coronal brain slices from 14-month-old mice (A, C) WT and (B, D) 5xFAD mice were stained with antibodies against GFAP (green) and C1q (red) and co-stained with Congo red for A β plaques (white). (C–D) Orthogonal slices of z-stacks showing co-localized astrocyte processes with C1q around plaques. Co-localization appears yellow and is indicated by arrows. Scale bar represents 20 μ m in A–B and 10 μ m in C–D (n = 3). (E) C1qA expression levels in cortex homogenates from WT and 5xFAD mice at 2, 6, 9 and 12-month-old mice (n = 3 in each group, *p < 0.05, ***p < 0.001). (F) Confocal images of old 5xFAD astrocytes stained with antibodies against GFAP (green), C1q (red) and DAPI (blue) showing C1q expression within astrocytes (yellow for colocalization in the merged image). Scale represents 20 μ m. (G–H) C1qA levels were measured by RT-PCR in astrocyte cultures from (G) 3-month-old (H) 12-month-old WT and 5xFAD mice. N = 9 per group, cultured from 3 independent mice run in triplicates.

have a reduced expression of genes involved in neuronal support (Orre et al., 2014a). One such gene was vascular endothelial growth factor a (VEGFa). Therefore, we measured VEGFa gene expression in our cultured cells and found a substantial decrease of 64% in old 5xFAD astrocytes compared to old WT astrocytes (p < 0.001, Fig. 6D). This seems to be specific for VEGFa, as transcription levels of other neurotrophic factors such as brain derived neurotrophic factor (BDNF) and neurotrophin-3 (NTF3) were not altered in old 5xFAD astrocytes.

A reduction in neuronal support by old 5xFAD astrocytes could be due to direct cell-to-cell interactions or secreted factors transferred through the medium. To further characterize the difference in astrocyte-secreted factors, we induced oxidative stress in neuronal cells and let the neurons recover in conditioned medium from either old WT or 5xFAD astrocytes for 24 h. Interestingly, while old WT astrocyte-conditioned medium did not affect neuronal viability in this assay, incubation with old 5xFAD astrocyte-conditioned media resulted

in further neuronal loss of approximately 15% (Fig. 6E). One of the pro-inflammatory cytokines secreted by astrocytes that might lead to neuronal death is Interleukin 6 (IL-6) (Van Wagoner et al., 1999). We measured IL-6 transcript by RT-PCR and found a significant increase of ~3-fold in old 5xFAD over WT astrocytes (*p < 0.05) (Fig. 6F). To measure IL-6 cytokine secretion we stimulated old astrocytes with Polyinosinic:polycytidylic acid (Poly I:C) (Park et al., 2006), as basal IL-6 secretion levels were undetected in both WT and 5xFAD. After 24 h, we found that old 5xFAD astrocytes showed an increase of 4.3-fold in IL-6 secretion as compared to old WT astrocytes (Fig. 6G).

4. Discussion

In this research, we discovered that adult astrocytes isolated from old 5xFAD mice show impairment in clearing A β and in neuronal support as compared to age-matched control astrocytes. Furthermore, we

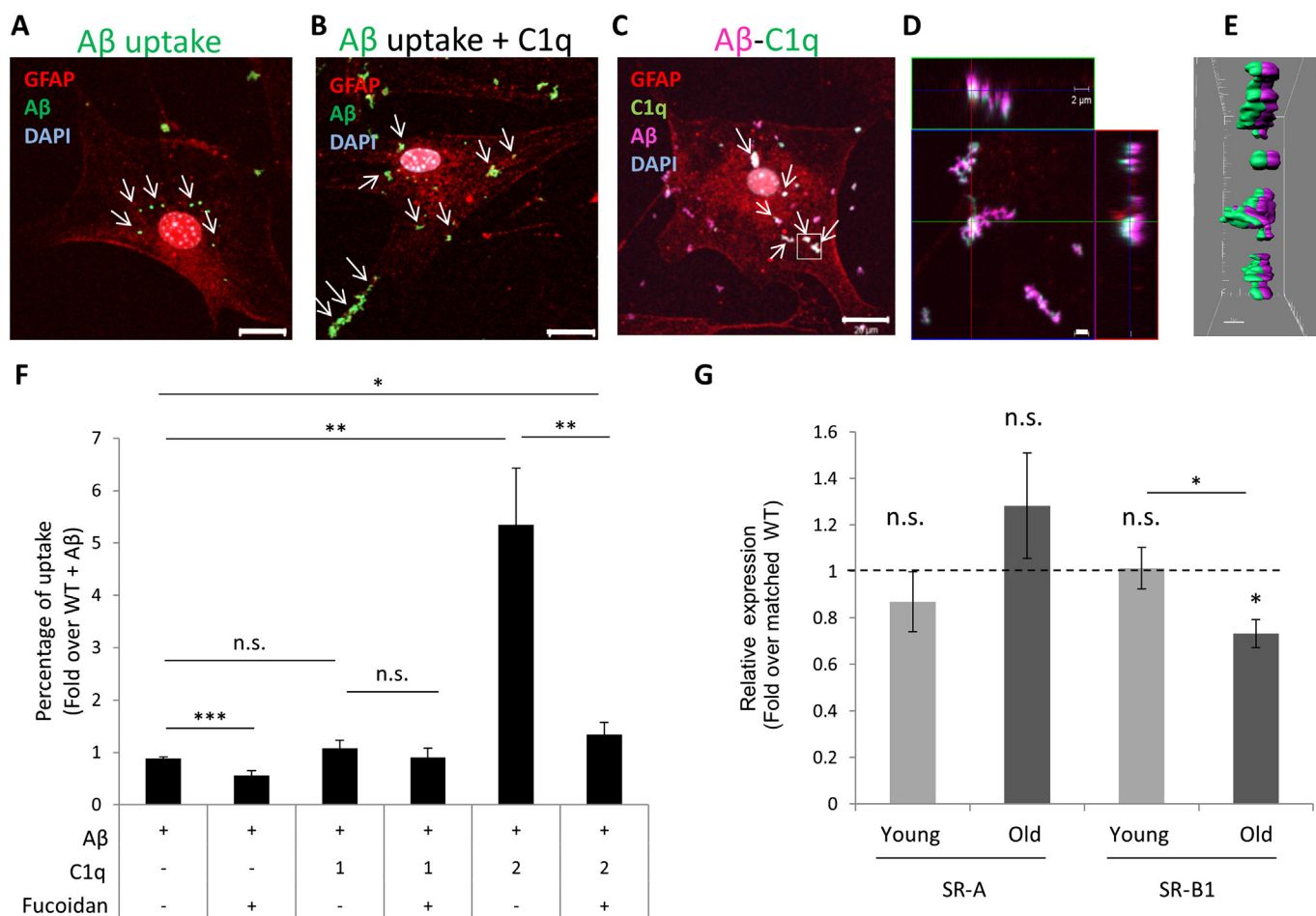


Fig. 5. C1q enhances A β uptake by astrocytes through a scavenger receptor-dependent pathway. (A–E) 0.2 μ M Alexa-488 labeled A β 42 (green) was pre-incubated with (A) control buffer or (B) 10 μ g/ml C1q at 37 $^{\circ}$ C for 30 min and placed on old 5xFAD astrocyte cultures for 16 h. (C–E) similar experiment as in (A–B) with 10 μ g/ml C1q-5-FAM (green) and 0.2 μ M Alexa-647 labeled A β 42 (magenta). (D) Orthogonal image of enlargement of indicated white square in (C). (E) Representative surface rendering of (D) obtained by IMARIS. Scale bar represents 2 μ m. (F) Old WT and 5xFAD astrocytes were pre-incubated with fucoidan (100 μ g/ml) for 30 min prior to addition of A β with or without C1q (concentrations indicated in the graph) for 2 h. Uptake was measured by Flow cytometry. (n = 4–14, from 6 independent experiments). Measurement of SR-B1 mRNA expression levels in young WT (n = 4) and 5xFAD (n = 6) astrocytes by RT-PCR (run in triplicates). (G) Measurement of SR-A and SR-B1 mRNA expression levels in young WT (n = 9), young 5xFAD (n = 9), old WT (n = 9–13) and old 5xFAD (n = 12–14) astrocytes by RT-PCR (Five independent experiments run in triplicates). Broken line represents normalized WT age matched control. Bars represent mean + SEM, *p < 0.05, **p < 0.01, ***p < 0.001, n.s. – not significant.

determined a role for C1q in the enhancement of A β uptake by astrocytes.

We presented and characterized a protocol for culture of adult mouse astrocytes. These cells proliferate for up to three weeks in culture and reach 20–30 times the initial cell number, thus enabling us to conduct more complex experiments with increased power and robust results. To date, several astrocyte specific genes have been used for direct isolation of astrocytes from the adult mouse brain. This was accomplished by cell sorting of astrocytes from GFAP (Brenner et al., 1994), S100 β , GLAST1 (Regan et al., 2007), GLT1 (Regan et al., 2007; Yang et al., 2011) and ALDH1L1 (Yang et al., 2011; Zamanian et al., 2012) transgenic reporter mice or by antibodies against cell-surface proteins such as GLT1 (Orre et al., 2014b). However, most of these promoters have been shown to be affected in AD mouse models, leading to differences in expression, and introducing possible biases in the isolation process (Orre et al., 2014a). Another approach, developed by Barres and colleagues, uses multiple immunopanning steps targeted at cell specific cell-surface markers of various CNS cells from mice (Foo et al., 2011) and human brains (Zhang et al., 2015). For isolation of astrocytes, they elegantly used an astrocyte-specific integrin (integrin beta 5) or anti-Hepa CAM, an astrocyte specific cell-adhesion glycoprotein (Foo et al., 2011). Nevertheless, different pathological states might affect the expression levels of those markers in astrocytes. Our protocol

enables culturing highly enriched adult astrocytes from different ages without using specific isolation markers that could be differentially expressed during disease progression.

Astrocyte activation, as demonstrated by increased GFAP expression, has a substantial impact on the consequences of an insult or disease state (Maragakis and Rothstein, 2006). In AD patients and AD mouse models, there is a significant elevation of GFAP in astrocytes surrounding A β plaques. In our astrocyte cultures, old 5xFAD astrocytes maintain higher GFAP mRNA and protein expression as compared to WT astrocytes for two weeks in culture. Of note, knockout of GFAP in an AD mouse model resulted in a 2-fold increase in plaque burden and twice the amount of dystrophic neurites (Kraft et al., 2013). These experiments demonstrate that improper astrocyte activation in AD might lead to impairments in A β clearance and to neurodegeneration. Interestingly, when microglial cells were ablated from an AD mouse model, there was a significant elevation of astrocytes reactivity around plaques and the A β load was not affected (Grathwohl et al., 2009). Thus, a complex interplay between glial cells and neurons is needed to react efficiently to the pathological environment.

C1q is composed of 18 polypeptide chains with six repeats of three different polypeptides; C1qA, C1qB and C1qC (Kishore and Reid, 2000). We demonstrated an increase in the expression of C1qA in 5xFAD cortex homogenates and specifically by old 5xFAD astrocytes as

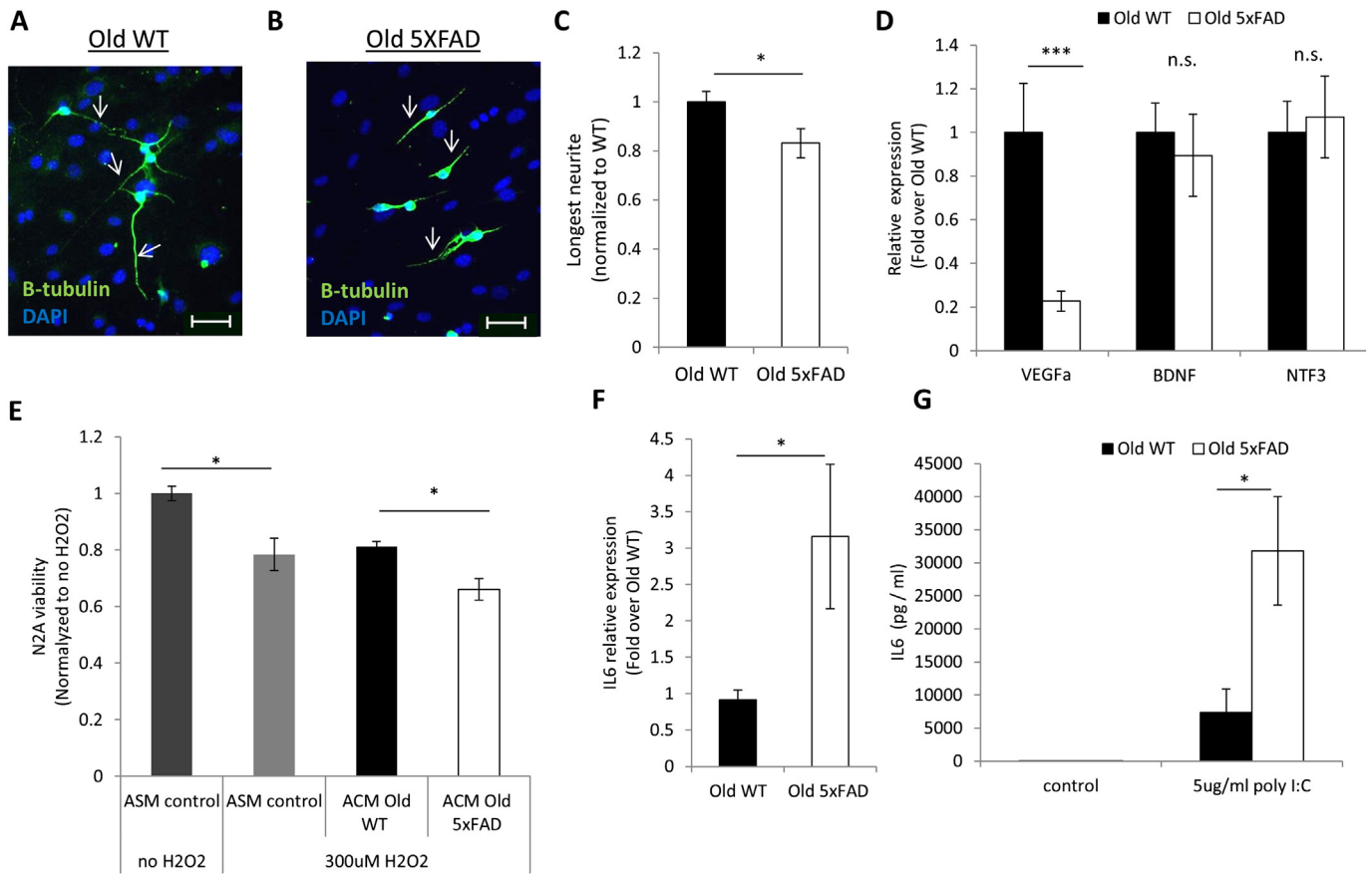


Fig. 6. Old 5xFAD astrocytes show impairment in supporting neuronal growth. Neonatal neurons were plated on old (A) WT and (B) 5xFAD astrocyte cultures for 24 h, then fixed and stained with mouse anti- β -tubulin to stain neurons, and DAPI to stain cell nuclei. (C) Longest neurite in each neuron was measured in at least 100 neurons per coverslip and averaged ($n = 11-16$), three experiments done in duplicates from 4 to 5 mice per group. (D) Measurement of VEGFa, BDNF and NTF3 mRNA expression levels in old WT ($n = 7$) and 5xFAD ($n = 8$) astrocytes by RT-PCR (three independent experiments run in triplicates). (E) N2A neuroblastoma cell line was stimulated with 300 μ M H₂O₂ for 4 h in serum free medium then incubated for 24 h with serum free astrocyte conditioned medium (ACM) from old WT or 5xFAD astrocytes. Cell viability was assessed by methylene blue staining. Non-conditioned serum-free astrocyte medium (ASM) was used in control conditions (One-way ANOVA, $n = 6$, in two independent experiments done in triplicates). (F) Measurement of IL6 mRNA expression levels in old WT ($n = 18$) and 5xFAD ($n = 21$) astrocytes by RT-PCR (six independent experiments from 8 mice/group, run in triplicates). (G) IL-6 secreted to medium 24 h after stimulation with 5 μ g/ml Poly I:C were measured by ELISA. Baseline levels were undetected ($n = 6-7$ mice per group, run in three independent experiments).

compared to old WT astrocytes. Astrocytes were shown to express C1q under pathological conditions in patients with multiple sclerosis (Ingram et al., 2014) and temporal lobe epilepsy (Aronica et al., 2007) and also in AD mouse models (Orre et al., 2014a). Our immunofluorescence analysis showed that C1q expression is highly elevated around A β plaques in regions of the astrocytes' engagement with the plaques. It was recently reported that C1q protein levels are increased substantially in the brains of normal aged mice and humans in brain regions that are linked to the etiology AD, such as the hippocampus (Stephan et al., 2013). Interestingly, it was recently reported that CR1, a receptor that recognizes C1q and was recently reported to be linked to AD, is expressed mainly on astrocytes in AD (Fonseca et al., 2016). In this work, we suggest that C1q plays an important role in A β uptake by astrocytes. This is supported by its co-localization with astrocytes in the vicinity of A β plaques in the cortex of old 5xFAD mice. Of interest, *in vitro* incubation with C1q elevated A β uptake by 5xFAD astrocytes. Here we suggest that the elevation in C1q uptake is attributed to SR-B1 as shown by using fucoidan, a scavenger receptor inhibitor (Ravichandran and Lorenz, 2007). Additionally, the observed significant reduction in SR-B1 in 5xFAD astrocytes that may account for the reduction in the A β uptake impairment in old 5xFAD astrocytes, even in an environment where C1q is abundant.

Previous research highlighted the importance of scavenger receptors such as SR-B1 in A β phagocytosis and degradation (Alarcon et al., 2005; Mulder et al., 2012; Wyss-Coray et al., 2003; Frenkel et al., 2013). While young 5xFAD astrocytes did not differ in their ability to uptake A β as

compared to young WT astrocytes, we observed a reduced uptake in old 5xFAD astrocytes. This suggests a progressive defect that might be acquired throughout long exposure to the diseased environment. In addition, we discovered that impairment in A β uptake in old 5xFAD astrocytes was correlated with lower expression of the scavenger receptor SR-B1. Studies by Neilsen et al., demonstrated that human astrocytes are capable of A β uptake *in vitro* depending on A β conformation and combination with several amyloid-associated proteins (AAP) (Nielsen et al., 2010; Nielsen et al., 2009). They reported that stimulation of astrocytes from non-demented brains with A β 42 combined with several APPs resulted in upregulation of SR-B1. Of note, human AD-derived astrocytes did not upregulate SR-B1 following A β 42 stimulation, indicating a possible impairment in astrocyte-mediated A β clearance in human AD brains (Mulder et al., 2012). Another line of evidence suggests that failure of astrocyte intracellular vesicle transport carrying the PS1 mutation might underlie defects in astrocytic A β clearance (Stenovec et al., 2015). Moreover, enhancing lysosomal biogenesis in astrocytes in an AD mouse model attenuated plaque pathogenesis (Xiao et al., 2014). These experiments call for therapies targeted at restoring phagocytic pathways in astrocytes.

Our data further demonstrate astrocytic impairment in neuronal support in the functional level, as old 5xFAD astrocytes induced less neurite growth when co-cultured with neonatal neurons compared to old WT astrocytes. We suggest that this impairment is linked to a significant reduction of ~65% in VEGFa expression by old 5xFAD astrocytes. VEGF is mainly known for its angiogenic effects on endothelial cells

(Neufeld et al., 1994) and is considered to be associated with detrimental aspects of AD progression (Wood et al., 2015). However, it was also shown to induce neuronal growth (Sondell et al., 1999; Sondell et al., 2000) and promote neuroprotection following various insults, such as ischemia and glucose deprivation (Jin et al., 2000). Notably, a detailed immunostaining analysis of VEGF during normal aging found lower VEGF expression in GFAP-positive astrocytes with normal aging (Bernal and Peterson, 2011). Thus, lower VEGFa expression by old 5xFAD astrocytes may account for the neuronal growth defects found in our co-culture experiments.

We discovered that old 5xFAD astrocytes secreted ~4-fold more IL-6 than old WT astrocytes. High levels of IL-6 were measured in post-mortem AD brains, and were shown to be highly expressed in activated human astrocytes in the disease (Huell et al., 1995; Sokolova et al., 2009; Van Wagoner et al., 1999). In addition, mice overexpressing IL-6 under the astrocytic GFAP promoter developed severe neurodegeneration, astrogliosis and major neuronal defects such as seizures (Campbell et al., 1993). Detailed analysis of the composition of factors secreted from WT and AD astrocytes is needed to gain a better understanding of mechanisms by which astrocytes might affect neuronal survival in AD.

It was previously suggested that the expression of AD-related genes such as PS1 might affect microglia (Farfara et al., 2011) and astrocyte activation (Stenovec et al., 2015). However, in 5xFAD mice, all five familial AD mutations are expressed under the Thy1 neuronal promoter (Oakley et al., 2006). Therefore, it was expected that astrocyte reactivity would be similar to WT, once the cells are cultured outside the brain's microenvironment. However, alterations in GFAP levels and in functional A β clearance remained even after 2–3 weeks in culture. One possibility is that throughout exposure to the diseased environment, astrocytes underwent irreversible epigenetic changes that affected their gene expression and function. Interestingly, a study that compared histone modifications in astrocytes from adult and middle-aged rats following ischemia found reduced chromatin activity associated with significant changes in the VEGF pathway activation in astrocytes isolated from middle-aged rats compared to young adult rats. They concluded that the age-dependent decline in VEGF might account for the reduced neuroprotection and increased vulnerability to ischemia in the middle-aged rats (Chisholm et al., 2015). In line with those results, we found a reduction in VEGFa expression in astrocytes from old AD mouse brains *versus* control.

In conclusion, we suggest here that environmental-induced pathological changes in astrocyte activity during the progression of AD may reduce A β clearance and accelerate neurodegeneration.

Supplementary data to this article can be found online at <http://dx.doi.org/10.1016/j.nbd.2016.08.001>.

Disclosure statement

All authors declare no biomedical financial interests or conflicts of interest in this study.

Author contributions

T.I. and D.F. conceived and planned the experiments and analyzed the data, T.I. executed all the experiments, D.K. performed together with T.I. the *in vivo* imaging experiments with the supervision of P.B. and T.I. and D.F. wrote the manuscript. D.T., S.K. and R.G. assisted with co-culture experiments and data analysis. P.B., A.B., Z.F. and R.V. assisted in critical reading and discussion.

Acknowledgements

This study was supported by a grant from the Israeli Ministry of Science Technology and Space to D.F. T.I. is the recipient of a scholarship from the Clore Israel Foundation. We wish to thank Ronit Shapira for

her assistance with the mouse colony. We also wish to thank Dr. Orit Sagi-Assif for technical assistance with flow cytometry experiments, Dr. Anat Nitzan for technical assistance with confocal microscopy and Dr. Yael Zilberstien for assistance with image analysis.

References

- Alarcon, R., et al., 2005. Expression of scavenger receptors in glial cells. Comparing the adhesion of astrocytes and microglia from neonatal rats to surface-bound beta-amyloid. *J. Biol. Chem.* 280, 30406–30415.
- Aronica, E., et al., 2007. Complement activation in experimental and human temporal lobe epilepsy. *Neurobiol. Dis.* 26, 497–511.
- Attwell, D., et al., 2010. Glial and neuronal control of brain blood flow. *Nature.* 468, 232–243.
- Bateman, R.J., et al., 2006. Human amyloid-beta synthesis and clearance rates as measured in cerebrospinal fluid in vivo. *Nat. Med.* 12, 856–861.
- Bernal, G.M., Peterson, D.A., 2011. Phenotypic and gene expression modification with normal brain aging in GFAP-positive astrocytes and neural stem cells. *Aging Cell* 10, 466–482.
- Braak, H., et al., 1993. Staging of Alzheimer-related cortical destruction. *Eur. Neurol.* 33, 403–408.
- Brenner, M., et al., 1994. GFAP promoter directs astrocyte-specific expression in transgenic mice. *J. Neurosci.* 14, 1030–1037.
- Cahoy, J.D., et al., 2008. A transcriptome database for astrocytes, neurons, and oligodendrocytes: a new resource for understanding brain development and function. *J. Neurosci.* 28, 264–278.
- Campbell, I.L., et al., 1993. Neurologic disease induced in transgenic mice by cerebral overexpression of interleukin 6. *Proc. Natl. Acad. Sci. U. S. A.* 90, 10061–10065.
- Chisholm, N.C., et al., 2015. Histone methylation patterns in astrocytes are influenced by age following ischemia. *Epigenetics* 10, 142–152.
- Eikelenboom, P., Stam, F.C., 1984. An immunohistochemical study on cerebral vascular and senile plaque amyloid in Alzheimer's dementia. *Virchows Arch. B Cell Pathol. Incl. Mol. Pathol.* 47, 17–25.
- Farfara, D., et al., 2011. Gamma-secretase component presenilin is important for microglia beta-amyloid clearance. *Ann. Neurol.* 69, 170–180.
- Fonseca, M.I., et al., 2004. Absence of C1q leads to less neuropathology in transgenic mouse models of Alzheimer's disease. *J. Neurosci.* 24, 6457–6465.
- Fonseca, M.I., et al., 2016. Analysis of the putative role of C1r in Alzheimer's disease: genetic association, expression and function. *PLoS One* 11, e0149792.
- Foo, L.C., et al., 2011. Development of a method for the purification and culture of rodent astrocytes. *Neuron* 71, 799–811.
- Fraser, D.A., et al., 2010. C1q enhances microglial clearance of apoptotic neurons and neuronal blebs, and modulates subsequent inflammatory cytokine production. *J. Neurochem.* 112, 733–743.
- Frenkel, D., et al., 2013. Scara1 deficiency impairs clearance of soluble amyloid-beta by mononuclear phagocytes and accelerates Alzheimer's-like disease progression. *Nat. Commun.* 4, 2030.
- Gdalyahu, A., et al., 2012. Associative fear learning enhances sparse network coding in primary sensory cortex. *Neuron* 75, 121–132.
- Goldman, J.S., et al., 2002. Very early-onset familial Alzheimer's disease: a novel presenilin 1 mutation. *Int. J. Geriatr. Psychiatry* 17, 649–651.
- Grathwohl, S.A., et al., 2009. Formation and maintenance of Alzheimer's disease beta-amyloid plaques in the absence of microglia. *Nat. Neurosci.* 12, 1361–1363.
- Huell, M., et al., 1995. Interleukin-6 is present in early stages of plaque formation and is restricted to the brains of Alzheimer's disease patients. *Acta Neuropathol.* 89, 544–551.
- Husemann, J., et al., 2002. Scavenger receptors in neurobiology and neuropathology: their role on microglia and other cells of the nervous system. *Glia* 40, 195–205.
- Ingram, G., et al., 2014. Complement activation in multiple sclerosis plaques: an immunohistochemical analysis. *Acta Neuropathol. Commun.* 2, 53.
- Iram, T., Frenkel, D., 2012. Targeting the role of astrocytes in the progression of Alzheimer's disease. *Curr. Signal Transduction Ther.* 7, 20–27.
- Iram, T., et al., 2016. Megf10 is a receptor for C1Q that mediates clearance of apoptotic cells by astrocytes. *J. Neurosci.* 36, 5185–5192.
- Jiang, H., et al., 1994. Beta-amyloid activates complement by binding to a specific region of the collagen-like domain of the C1q A chain. *J. Immunol.* 152, 5050–5059.
- Jin, K.L., et al., 2000. Vascular endothelial growth factor: direct neuroprotective effect in *in vitro* ischemia. *Proc. Natl. Acad. Sci. U. S. A.* 97, 10242–10247.
- Kishore, U., Reid, K.B., 2000. C1q: structure, function, and receptors. *Immunopharmacology* 49, 159–170.
- Kofuji, P., Newman, E.A., 2004. Potassium buffering in the central nervous system. *Neuroscience* 129, 1045–1056.
- Kraft, A.W., et al., 2013. Attenuating astrocyte activation accelerates plaque pathogenesis in APP/PS1 mice. *FASEB J.* 27, 187–198.
- Kulijewicz-Nawrot, M., et al., 2012. Astrocytic cytoskeletal atrophy in the medial prefrontal cortex of a triple transgenic mouse model of Alzheimer's disease. *J. Anat.* 221, 252–262.
- Lavi, A., et al., 2014. DOC2B and Munc13-1 differentially regulate neuronal network activity. *Cereb. Cortex* 24, 2309–2323.
- Lifshitz, V., et al., 2013. Scavenger receptor A deficiency accelerates cerebrovascular amyloidosis in an animal model. *J. Mol. Neurosci.* 50, 198–203.
- Maragakis, N.J., Rothstein, J.D., 2006. Mechanisms of disease: astrocytes in neurodegenerative disease. *Nat. Clin. Pract. Neurol.* 2, 679–689.

- Mawuenyega, K.G., et al., 2010. Decreased clearance of CNS beta-amyloid in Alzheimer's disease. *Science* 330, 1774.
- McGeer, P.L., McGeer, E.G., 2002. The possible role of complement activation in Alzheimer disease. *Trends Mol. Med.* 8, 519–523.
- Mulder, S.D., et al., 2012. The effect of amyloid associated proteins on the expression of genes involved in amyloid-beta clearance by adult human astrocytes. *Exp. Neurol.* 233, 373–379.
- Neufeld, G., et al., 1994. Vascular endothelial growth factor and its receptors. *Prog. Growth Factor Res.* 5, 89–97.
- Nguyen, Q.T., et al., 2009. MPScope 2.0: a computer system for two-photon laser scanning microscopy with concurrent plasma-mediated ablation and electrophysiology. In: Frostig, R.D. (Ed.), *In Vivo Optical Imaging of Brain Function* Boca Raton (FL).
- Nielsen, H.M., et al., 2009. Binding and uptake of A beta1–42 by primary human astrocytes in vitro. *Glia* 57, 978–988.
- Nielsen, H.M., et al., 2010. Astrocytic A beta 1–42 uptake is determined by A beta-aggregation state and the presence of amyloid-associated proteins. *Glia* 58, 1235–1246.
- Nimmerjahn, A., Helmchen, F., 2012. In vivo labeling of cortical astrocytes with sulforhodamine 101 (SR101). *Cold Spring Harb. Protoc.* 2012, 326–334.
- Nimmerjahn, A., et al., 2004. Sulforhodamine 101 as a specific marker of astroglia in the neocortex in vivo. *Nat. Methods* 1, 31–37.
- Oakley, H., et al., 2006. Intraneuronal beta-amyloid aggregates, neurodegeneration, and neuron loss in transgenic mice with five familial Alzheimer's disease mutations: potential factors in amyloid plaque formation. *J. Neurosci.* 26, 10129–10140.
- Olabarria, M., et al., 2010. Concomitant astroglial atrophy and astrogliosis in a triple transgenic animal model of Alzheimer's disease. *Glia* 58, 831–838.
- Orre, M., et al., 2014a. Isolation of glia from Alzheimer's mice reveals inflammation and dysfunction. *Neurobiol. Aging* 35, 2746–2760.
- Orre, M., et al., 2014b. Acute isolation and transcriptome characterization of cortical astrocytes and microglia from young and aged mice. *Neurobiol. Aging* 35, 1–14.
- Park, C., et al., 2006. TLR3-mediated signal induces proinflammatory cytokine and chemokine gene expression in astrocytes: differential signaling mechanisms of TLR3-induced IP-10 and IL-8 gene expression. *Glia* 53, 248–256.
- Pellerin, L., et al., 2007. Activity-dependent regulation of energy metabolism by astrocytes: an update. *Glia* 55, 1251–1262.
- Ravichandran, K.S., Lorenz, U., 2007. Engulfment of apoptotic cells: signals for a good meal. *Nat. Rev. Immunol.* 7, 964–974.
- Regan, M.R., et al., 2007. Variations in promoter activity reveal a differential expression and physiology of glutamate transporters by glia in the developing and mature CNS. *J. Neurosci.* 27, 6607–6619.
- Rothstein, J.D., et al., 1996. Knockout of glutamate transporters reveals a major role for astroglial transport in excitotoxicity and clearance of glutamate. *Neuron* 16, 675–686.
- Schafer, D.P., et al., 2012. Microglia sculpt postnatal neural circuits in an activity and complement-dependent manner. *Neuron* 74, 691–705.
- Schafer, D.P., et al., 2014. An engulfment assay: a protocol to assess interactions between CNS phagocytes and neurons. *J. Vis. Exp.*
- Sofroniew, M.V., 2009. Molecular dissection of reactive astrogliosis and glial scar formation. *Trends Neurosci.* 32, 638–647.
- Sofroniew, M.V., Vinters, H.V., 2010. Astrocytes: biology and pathology. *Acta Neuropathol.* 119, 7–35.
- Sokolova, A., et al., 2009. Monocyte chemoattractant protein-1 plays a dominant role in the chronic inflammation observed in Alzheimer's disease. *Brain Pathol.* 19, 392–398.
- Sondell, M., et al., 1999. Vascular endothelial growth factor has neurotrophic activity and stimulates axonal outgrowth, enhancing cell survival and Schwann cell proliferation in the peripheral nervous system. *J. Neurosci.* 19, 5731–5740.
- Sondell, M., et al., 2000. Vascular endothelial growth factor is a neurotrophic factor which stimulates axonal outgrowth through the flk-1 receptor. *Eur. J. Neurosci.* 12, 4243–4254.
- Stellwagen, D., Malenka, R.C., 2006. Synaptic scaling mediated by glial TNF-alpha. *Nature* 440, 1054–1059.
- Stenovec, M., et al., 2015. Expression of familial Alzheimer disease presenilin 1 gene attenuates vesicle traffic and reduces peptide secretion in cultured astrocytes devoid of pathologic tissue environment. *Glia*.
- Stephan, A.H., et al., 2013. A dramatic increase of C1q protein in the CNS during normal aging. *J. Neurosci.* 33, 13460–13474.
- Thal, D.R., et al., 2000. Amyloid beta-protein (Abeta)-containing astrocytes are located preferentially near N-terminal-truncated Abeta deposits in the human entorhinal cortex. *Acta Neuropathol.* 100, 608–617.
- Trudler, D., et al., 2014. DJ-1 deficiency triggers microglia sensitivity to dopamine toward a pro-inflammatory phenotype that is attenuated by rasagiline. *J. Neurochem.* 129, 434–447.
- Van Wagoner, N.J., et al., 1999. Interleukin-6 (IL-6) production by astrocytes: autocrine regulation by IL-6 and the soluble IL-6 receptor. *J. Neurosci.* 19, 5236–5244.
- Verkhatsky, A., et al., 2014. Glial asthenia and functional paralysis: a new perspective on neurodegeneration and Alzheimer's disease. *Neuroscientist.*
- Wood, L.B., et al., 2015. Identification of neurotoxic cytokines by profiling Alzheimer's disease tissues and neuron culture viability screening. *Sci. Rep.* 5, 16622.
- Wyss-Coray, T., et al., 2003. Adult mouse astrocytes degrade amyloid-beta in vitro and in situ. *Nat. Med.* 9, 453–457.
- Xiao, Q., et al., 2014. Enhancing astrocytic lysosome biogenesis facilitates Abeta clearance and attenuates amyloid plaque pathogenesis. *J. Neurosci.* 34, 9607–9620.
- Yamazaki, S., Onishi, E., Enami, K., Natori, K., Kohase, M., Sakamoto, H., Tanouchi, M., Hayashi, H., 1986. Proposal of standardized methods and reference for assaying recombinant human tumor necrosis factor. *Jpn. J. Med. Sci. Biol.* 39, 105–118.
- Yang, Y., et al., 2011. Molecular comparison of GLT1⁺ and ALDH1L1⁺ astrocytes in vivo in astroglial reporter mice. *Glia* 59, 200–207.
- Yeh, C.Y., et al., 2011. Early astrocytic atrophy in the entorhinal cortex of a triple transgenic animal model of Alzheimer's disease. *ASN Neuro* 3, 271–279.
- Zamanian, J.L., et al., 2012. Genomic analysis of reactive astrogliosis. *J. Neurosci.* 32, 6391–6410.
- Zhang, Y., et al., 2015. Purification and characterization of progenitor and mature human astrocytes reveals transcriptional and functional differences with mouse. *Neuron.*